

Current image tunneling spectroscopy of boron-doped nanodiamonds

Hsiu-Fung Cheng

Department of Physics, National Taiwan Normal University, 88 Ting-Chou Road, Sec. 4, Taipei, Taiwan 116, Republic of China

Yen-Chih Lee and Su-Jien Lin

Department of Materials Science and Engineering, National Tsing Hua University, 101, Kuang-Fu Road, Sec. 2, Hsin-Chu, Taiwan 300, Republic of China

Yi-Ping Chou and Tom T. Chen

Department of Physics, National Tsing Hua University, 101, Kuang-Fu Road, Sec. 2, Hsin-Chu, Taiwan 300, Republic of China

I-Nan Lin^{a)}

Department of Physics, Tamkang University, 151 Ying-Chuan Road, Tamsui, Taiwan 251, Republic of China

(Received 25 August 2004; accepted 25 October 2004; published online 26 January 2005)

The electron field emission properties of the nanodiamond films were examined using scanning tunneling microscopic (STM) technique. Current image tunneling spectroscopic measurements reveal the direct dependence of electron tunneling/field emission behavior of the films on the proportion of grain boundaries present. Local tunneling current-voltage (I_t - V) measurements show that incorporation of boron species insignificantly alters the occupied state, but markedly modifies the empty state of the diamond films, viz. it induces the presence of impurity states for the films heavily doped with borons, resulting in smaller emission energy gap for the samples. Such a characteristic improves both the local electron field emission behavior of the diamond films measured by STM and the average electron field emission properties measured by conventional parallel plate setup. These results infer clearly that the presence of impurity states due to boron doping is a prime factor improving the field emission properties for these boron-doped nanodiamond films. © 2005 American Institute of Physics. [DOI: 10.1063/1.1834722]

I. INTRODUCTION

Diamond films, which can be synthesized easily by using microwave plasma enhanced chemical vapor deposition (MPECVD) process have been extensively investigated for the applications as electron sources, since they possess very consistent and good electron field emission properties.¹⁻³ Even though the carbon nanotubes (CNTs) own superior electron field emission properties to the diamond films, the growth of CNTs is extremely sensitive to preparation of the catalysts such that the characteristics of the CNTs have poor consistency. Therefore, there has been wide interest in improving the electron field emission properties of diamond films recently. One of the possible routes for increasing the electron field emission capacity of diamond films is to increase the proportion of the grain boundary region, as it has been proposed that the grain boundaries contain a sp^2 bond⁴ and provide a conduction path for electrons, facilitating the electron field emission process. Increasing nucleation density is of critical importance for the purpose of synthesizing nanodiamonds. Various techniques have been applied to enhance the nucleation rate for growing diamond films.⁵⁻¹² Among these techniques, the bias enhanced nucleation (BEN) process is overwhelmingly advantageous to those pre-nucleation processes⁹⁻¹¹ and can achieve a very high nucleation density.⁸⁻¹² However, the understanding on how the

decrease in grain size and the addition of the dopants modify the materials characteristics and electron field emission properties of the diamonds is still in its infancy.

In this article, we adopted the bias enhanced technique for synthesizing boron-doped nanodiamonds. Scanning tunneling microscopy (STM) was used to examine the intrinsic parameters related to the electronic structure of the diamond films. The correlation of these parameters with the electron tunneling behavior of the films was discussed.

II. EXPERIMENTS

Diamond films were grown by a microwave plasma enhanced chemical vapor deposition process (MPECVD) using ASTex 5400 reactors.^{13,14} The CH_4/H_2 gases with a flow rate of 18 sccm/300 sccm were excited by 2500 W microwave power, where the total pressure in the chamber was maintained at 70 torr. The substrates, (100) p -type silicon with 10–50 Ω cm resistivity, were maintained at around 900 °C during the growth of diamond films. To grow boron doped diamond films, 1–4 sccm $B(OCH_3)_3$ was introduced into the chamber by bubbling the H_2 gas through the $B(OCH_3)_3$ liquid maintained at 10 °C. These samples were designated as B1–B4 diamond films, respectively. A large negative bias (–100 V) was applied to Si substrates in the nucleation stage to facilitate the formation of diamond nuclei on mirror smooth silicon surface and in the growth stage to maintain

^{a)}Electronic mail: inanlin@mail.tku.edu.tw

small diamond grains. The diamonds were grown under this condition for about 0.5 h to reach a thickness of about $0.5 \mu\text{m}$.

The morphology and structure of the diamond films were examined using scanning electron microscopy (Joel) and Raman spectroscopies (Renishaw), respectively. The electron field emission properties of the B-doped diamond films were measured using a parallel-plate setup. The anode, indium-tin-oxide coated glass was separated from the cathode, diamond films coated silicon, using $100 \mu\text{m}$ glass beads as spacer. The current-voltage (I - V) characteristics of the diamond films were measured by Keithley 237 electrometers. The current-voltage (I - V) properties of the diamond films were analyzed using Fowler-Nordheim (F-N) model.¹⁵ The turn-on field was defined by the intersection of the two straight lines extrapolated from low-voltage and high-voltage segments of the F-N plots. The effective work function ($\phi_e = \phi/\beta$), which is the ratio of true work function (ϕ) and field enhancement factor (β), of the diamond films can be deduced from the slope of the F-N plots.¹⁵

Moreover, to examine the local electron field emission properties of the diamond films, scanning tunneling microscopy (STM, Park Scientific Instruments, Auto-probe CP) with a PtIr-tip about 50 nm in diameter was used. The STM was first set at constant current mode (0.5 nA for 1.0 V tip-to-film voltage) for examining the morphology of the samples. The tunneling spectroscopy for a selected region of the films was then measured by sweeping the bias voltage applied to diamond films between ± 5 V, while the tip-to-film gap was kept at around 1 nm. To evaluate the localized electron field emission properties of the diamond films, the tip-to-film gap was increased to 5 nm to completely eliminate the tunneling current between the PtIr(Si)-tip and diamond films. An electron field emission spectrum was obtained by sweeping the tip-to-film voltage from 0 to -5 V, which was then analyzed using the Fowler-Nordheim model.¹⁵

III. RESULTS AND DISCUSSION

Figure 1(a) shows a typical diamond grain with B3 composition, which is of pyramidal geometry, about $1 \mu\text{m}$ in size, and consists of (100)- and (111)-type surfaces. To investigate the local electron tunneling/field emission behaviors of the diamond grain, the scanning area was divided into 64×64 segments and tunneling current-voltage (I_t - V) curves corresponding to each segment were acquired with the voltage swept in the range of ± 5 V. Figure 2 illustrates typical electron tunneling/field emission behavior, I_t - V curves, corresponding to the locations indicated in Fig. 1(b). The tunneling/field emission behavior changes dramatically among the locations on the surfaces. The (001)_A and (001)_B surfaces exhibit essentially no tunneling/field emission current, viz. these surfaces are essentially nonconductive [A and B, Fig. 2(a)], whereas the steps between these surfaces are very conductive, i.e., they show large tunneling/field emission current [step E in Fig. 1(b) and Fig. 2(b)]. The (111)_C flat surface and all the steps surrounding this surface (steps F, G, and H, Fig. 1(b)) are all very conductive. The electron

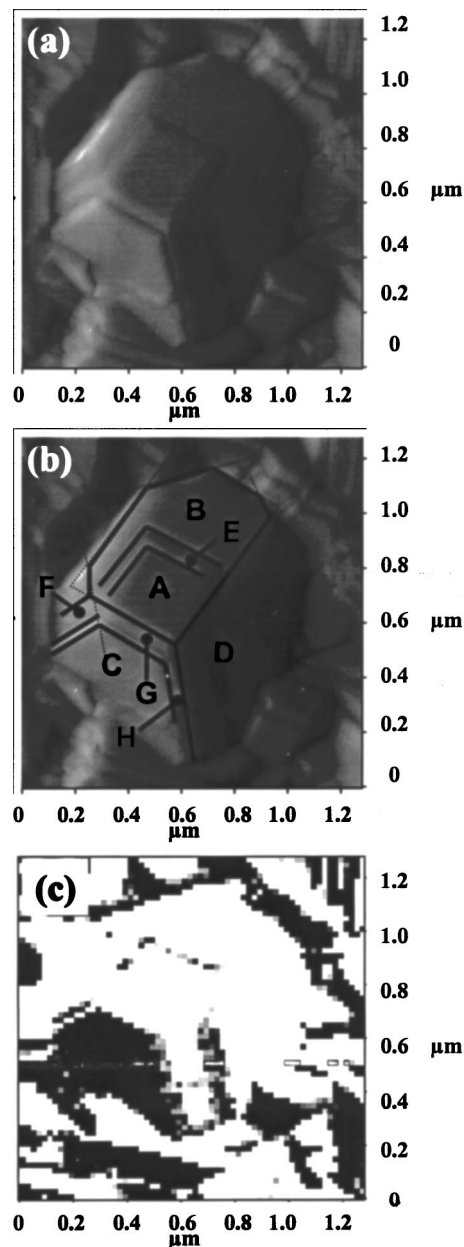


FIG. 1. (a) AFM micrograph of a typical diamond grain with pyramidal geometry, (b) the location of the tunneling current measurement, and (c) the current image tunneling spectroscopic (CITS) map of the pyramidal grains with the diamond films biased at -3.0 V [the darker spots represent larger electron field emission current from diamond films to PtIr(Si)-tip].

tunneling/field emission characteristics of the (111)_D surface vary with the locations as this surface contains many steps. It is interesting to observe that the segments tunneling better when the diamond films were positively biased also exhibit larger tunneling/field emitting capacity when they were negatively biased.

When the tunneling current (I_t) values of each segments is plotted for a given bias voltage, a current image tunneling spectroscopic (CITS) map, representing the distribution of the electron tunneling/field emission current of the diamond surface, is resulted. Figure 1(c) illustrates the CITS map for electrons emitted from diamond films to PtIr(Si)-tip, corresponding to $V_{e2} = -3.0$ V applied to diamond films. The darker spots represent larger electron tunneling/field emis-

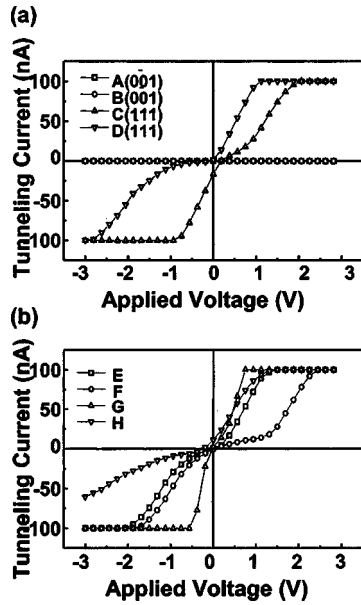


FIG. 2. The tunneling current–voltage (I_T – V) properties of (a) the flat surfaces of the pyramidal diamond grains and (b) the steps surrounding these flat surfaces, for the locations indicated in Fig. 1(b).

sion current. Contrary to the common knowledge that the corner, the joining of three surfaces, and the edges, the joining of two adjacent surfaces, emit more efficiently due to field concentration effect, Fig. 1(c) indicates that neither the corner nor the edge is emitting. It should be noted that the electrons emitted from diamond films in the negatively biased case include the tunneled and field-emitted ones.

The above-described results indicate that, even though the diamond films were boron-doped and were electrically conducting, it still requires good electron transport path, such as the steps, to supply sufficient amount of electrons to enhance field emission properties of the materials. Therefore, reducing the size of diamond grains so as to increase the proportion of grain boundaries seems to be a plausible route for improving the electron field emission properties for the diamond films, as the grain boundaries are highly defective and are expected to be a good conduction path for the electrons.

For the purpose of improving the electron field emission properties of the diamond materials, nanodiamonds doped with boron species were synthesized and their field emission properties were investigated. Typical atomic force microscope (AFM) micrograph of boron-doped nanodiamond films is shown in Fig. 3(a), indicating that the films contain a large number of nanosized diamond grains (~ 100 nm) distributed uniformly among the faceted diamond grains about 600 nm in size. The microstructure of the diamond films insignificantly varies with the boron content of the films. CITS map measured under -3.0 V bias in STM [Fig. 3(b)] illustrates that the electron tunneling/field emission behavior was greatly enhanced due to the presence of large proportion of grain boundaries in the nano-diamonds.

Figure 4(a) reveals that the Raman spectra of boron-doped nanodiamond films are predominated by a sharp D-band (1332 cm^{-1}) and a diffused D*-band ($\sim 1230\text{ cm}^{-1}$) resonance peaks, which represent, respectively, the faceted

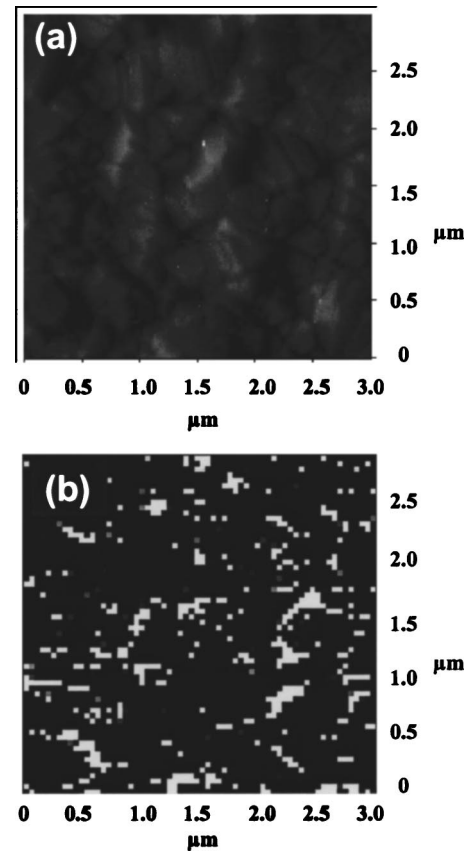


FIG. 3. (a) AFM micrograph of a typical nanodiamond films and (b) the current image tunneling spectroscopic (CITS) map of the nanodiamond films with the diamond films biased at -3.0 V [the darker spots represent larger field emission current from diamond films to P_T (Si)-tip].

and nanocrystalline diamonds. Increasing the boron doping level for these films do not alter the Raman spectra of the films, except that a small broaden Raman resonance peak representing amorphous carbons appears at around 1600 cm^{-1} (G^* -band) for most heavily doped samples (B4). While the microstructures and Raman spectroscopy of the diamond films vary insignificantly with the boron content in the films, the electron field emission properties of the diamond films are markedly changed due to the incorporation of boron species into the films. In Fig. 4(b), the electrical field dependence of the emission current density and the corresponding Fowler–Nordheim plots indicate that the B3 samples can be turned on at the smallest field, $(E_o)_{B3} = 8.8\text{ V}/\mu\text{m}$, and exhibits the largest electron field emission capacity, $(J_e)_{B3} = 250\text{ }\mu\text{A}/\text{cm}^2$. The boron doping enhances the electron field emission capacity of the diamond films without altering their turn-on field (E_o) and effective work function (ϕ_e), which are summarized in Table I(a).

To understand the genuine mechanism resulting in better electron field emission characteristics for B3 diamond films, the local electron tunneling behavior of the films were examined using scanning tunneling spectroscopy (STM). The tunneling spectra for a selected region of the diamond films were acquired by sweeping the bias voltage in the range of ± 5 V, while maintaining the tip-to-film distance at about 1 nm. Figures 5(a) and 5(b) show, respectively, the voltage dependency of the tunneling current characteristics (I_T – V)

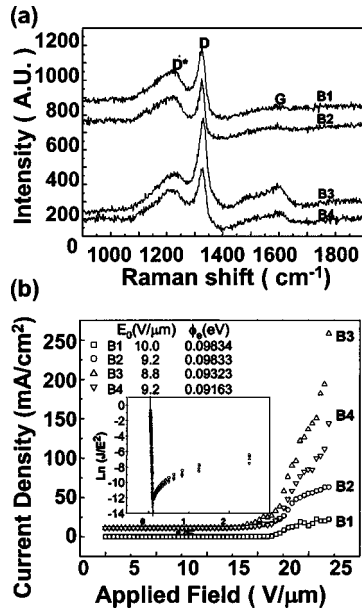


FIG. 4. (a) Raman spectroscopies and (b) electron field emission properties of nano-diamond films doped with 1–4 sccm $B(OCH_3)_3$ species, which were designated as B1–B4 [the inset in (b) shows Fowler–Nordheim plots of the I – V curves].

and the corresponding derivatives (dI_t/dV – V) for these boron-doped diamond films. The electrons tunnel from the tip to the films when the diamond films were positively biased. The maximum of the derivative curves is thus representing largest density of states (DOS) corresponding to the empty state for the diamond films. In contrast, the electrons tunnel from the films to the tip when the diamond films were negatively biased. The maximum of the derivative curves is thus representing the largest DOS corresponding to the occupied state for the diamond films. The separation between the two states represents the intermediate level (or the band gap) of the materials.

It is quite interesting to observe that, for the undoped sample [B₀, Fig. 5(b)], the empty state is located at around +3.52 V and the occupied state is located at around –2.1 V, resulting in an energy gap about $(E_g)_{B_0}=5.62$ eV, which is close to the reported band-gap value for undoped diamond films. Boron doping markedly modifies the DOS of empty

TABLE I. (a) The average electron field emission characteristics J_e and E_o , (b) the emission gap E_e , and (c) the local electron field emission behavior J'_e and E'_o , of boron-doped nanocrystalline diamond films.^a

Samples	B0	B1	B2	B3	B4
(a) $J_e(\mu A/cm^2)^b$	-	20.0	52.0	250.0	145.0
$E_o(V/\mu m)^b$	-	10.0	9.2	8.8	9.2
(b) $E_e(eV)^c$	-	4.8	3.78	2.27	2.84
(c) $J'_e(\mu A/cm^2)^d$	0.2	0.5	1.0	2.0	1.7
$E'_o(V/\mu m)^d$	49.8	43.4	39.0	18.5	47.3

^aDiamond films B0, B1, B2, B3, B4 were doped with 0–4 sccm $B(OCH_3)_3$.

^bElectron field emission characteristics measured by a parallel plate setup: J_e =emission current density and E_o =turn-on field.

^c E_e : Emission gap derived from (dI/dV) – V of tunneling current measured by STM.

^dLocal electron field emission characteristics: J'_e =emission current density and E'_o =turn-on field.

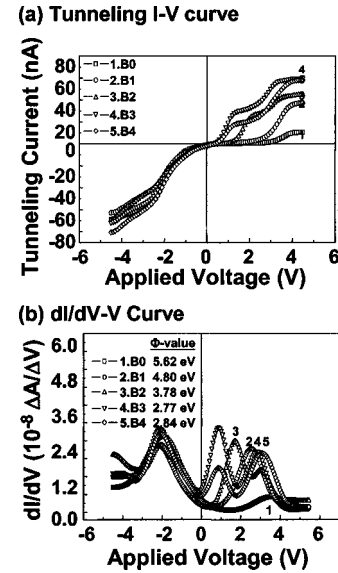


FIG. 5. (a) The tunneling current–voltage (I_t – V) characteristics and (b) the corresponding derivatives of tunneling current, dI_t/dV – V , for boron-doped nanodiamond films measured by STM techniques with tip-to-film gap set to at 1 nm.

states but insignificantly alters those of occupied state. For lightly doped samples (B1), only one empty state is observed ($E_e \sim 2.55$ eV), whereas for heavily doped ones (B2, B3, and B4), there exist two empty states ($E_e^1 \sim 2.85$ – 3.1 eV and $E_e^2 \sim 0.7$ – 1.2 eV). Since it is generally understood that the boron species are acceptors with the acceptor level close to the valence band ($E_a=0.3$ eV), these empty states are thus attributed to the formation of intermediate levels, designated as impurity states. The mechanism for the formation of intermediate state is still not clear. Probably, it has resulted from the induction of atomic defects, such as vacancies, due to the incorporation of large percentage of boron species.

The energy gap between occupied state and impurity state represents the energy barrier that the electrons need to overcome before they were field emitted, which is thus designated as emission gap (E_e). The energy level of impurity state shifts toward valence band as the boron content increases, resulting in a smaller emission gap. Table I(b) indicates that the impurity state, the E_e values, for B3 and B4 samples are markedly smaller than the E_e values for B1 and B2 samples. The implication of these results is that the boron species doped not only form acceptor levels, which enhance the electron transport in the diamond films, but may also induce the formation of impurity states, which facilitates the jump of electrons from valence band to conduction band. The electron field emission properties of the diamond films are thus markedly improved.

To investigate whether the presence of impurity levels really enhances the local electron field emission properties of the films, the tip-to-film gap was increased to about 5.0 nm to completely suppress the tunneling of electrons between the PtIr tip and diamond film. Only the electrons field emitted from the diamond films will be measured when the films were negatively biased. Figure 6 shows the local electron field-emission properties for the diamond films thus obtained. It is interesting to observe that tunneling current is

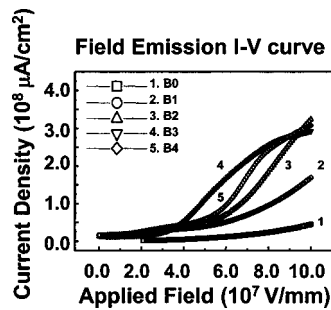


FIG. 6. The field emission current–voltage (I_e – V) characteristics for boron-doped nanodiamond films measured by STM technique with tip–to–film gap set at 5.0 nm.

insignificantly small when the diamond films were positively biased with respect to the PtIr tip, which suggest that the current measured under negative bias is the electrons field emitted from the diamond surface. The local electron field emission properties for the B-doped diamond films are listed in Table I(c), revealing that the electron field emission current density of the diamond films increases with the concentration of boron species incorporated into the films up to B3 samples and then decreases when over-doped, i.e., for B4 samples. The turn-on fields deduced from Fowler–Nordheim plots of Fig. 6 are also listed in Table I(c) to indicate that the B3 samples possess lowest turn-on field ($E'_o = 18.5 \text{ V}/\mu\text{m}$) and smallest effective work function ($\phi'_e = 0.07 \text{ eV}$). It should be noted that the applied field was calculated by simply dividing the voltage by the tip–to–film gap and the electron field emission current density was calculated by assuming that the emitting area is the same as the size of PtIr tip, i.e., 50 nm in diameter.

The localized electron field emission properties for the diamond films deduced from STM vary with the boron content of the films in a similar trend with the average electron field emission characteristics measured by parallel plate setup [cf. Tables I(a) and I(c)]. The undoped diamond films possess largest emission gap ($E_g = 5.62 \text{ eV}$) and require the largest electrical field to turn on the field emission ($E'_o = 49.8 \text{ V}/\mu\text{m}$), whereas the B3 diamond films own the smallest emission gap ($E_g = 2.27 \text{ eV}$) and need the smallest electrical field ($E'_o = 18.5 \text{ V}/\mu\text{m}$) to turn on the local field emission. These results infer that the local electron field emission characteristics for diamond films correlate with intrinsic electronic structure of the films intimately. The boron

doping affects the electron field emission properties of the diamond films mainly via the modification on the electronic structure of the films.

IV. CONCLUSION

The effect of boron doping on the electron field emission properties of the nanodiamond films was examined using STM technique. Tunneling current–voltage (I_t – V) characteristics measured by this technique indicate that the incorporation of a small proportion of boron species insignificantly alters the occupied state, but markedly modifies the empty state of diamond films. Furthermore, heavy boron doping induces the presence of the impurity state. Such a characteristic is closely related to the local electron field emission behavior of the diamond films measured by STM and the average electron field emission properties measured by conventional parallel plate setup.

ACKNOWLEDGMENTS

The authors gratefully acknowledge the National Science Council, R.O.C., for the financial support through Project No. NSC-93-2112-M-032-010 and No. NSC-93-2216-E-003-001.

- ¹C. A. Spindt, I. Brodie, L. Humphrey, and E. R. Westerberg, *J. Appl. Phys.* **47**, 5248 (1976).
- ²G. G. P. Van Gorkom and A. M. E. Hoeberechts, *J. Vac. Sci. Technol. B* **4**, 108 (1986).
- ³F. J. Himpsel, J. A. Knapp, and J. A. Van Vechten, *Phys. Rev. B* **20**, 624 (1979).
- ⁴W. Zhu, G. P. Kochanski, and A. E. White, *Appl. Phys. Lett.* **68**, 1157 (1995).
- ⁵T. K. Ku, S. H. Chen, and H. C. Cheng, *IEEE Electron Device Lett.* **17**, 208 (1996).
- ⁶J. W. Glesener and A. A. Morrish, *Appl. Phys. Lett.* **69**, 785 (1996).
- ⁷K. Okano, S. Koizumi, SRP. Silva, and G. Amaratunga, *Nature (London)* **381**, 140 (1996).
- ⁸K. Okano and K. K. Gleason, *Electron. Lett.* **31**(1), 74 (1995).
- ⁹M. W. Geis, J. C. Twichell, and T. M. Lyszczarz, *Appl. Phys. Lett.* **68**, 2294 (1996).
- ¹⁰T. M. Hong, S. H. Chen, Y. S. Chiou, and C. F. Chen, *Appl. Phys. Lett.* **67**, 2149 (1995).
- ¹¹W. Müller Seibert, E. Wörner, F. Fuchs, C. Wild, and P. Koidl, *Appl. Phys. Lett.* **68**, 759 (1996).
- ¹²J. H. Won, A. Hatta, H. Yagyu, N. Jiang, Y. More, T. Ito, T. Sasaki, and A. Hiraki, *Appl. Phys. Lett.* **68**, 2822 (1996).
- ¹³Y. H. Chen, C. T. Hu, and I. N. Lin, *J. Appl. Phys.* **84**, 3890 (1998).
- ¹⁴C. F. Shih, K. S. Liu, and I. N. Lin, *Diamond Relat. Mater.* **9**, 1591 (2000).
- ¹⁵A. Vander Ziel, *Solid State Physical Electronics* (Prentice-Hall, Englewood Cliffs, NJ, 1968), p. 144.